(12) INTERNATIONAL APPLICATION PUBLISHED UNDER THE PATENT COOPERATION TREATY (PCT)

(19) World Intellectual Property Organization
International Bureau

(43) International Publication Date
11 February 2010 (11.02.2010)

PCT

(10) International Publication Number
WO 2010/017524 A2

(51) **International Patent Classification**:
A61B 5/055 (2006.01)

(21) **International Application Number**:
PCT/US2009/053223

(22) **International Filing Date**:
7 August 2009 (07.08.2009)

(25) **Filing Language**: English

(26) **Publication Language**: English

(30) **Priority Data**:
61/087,111 7 August 2008 (07.08.2008) US

(71) **Applicant** *(for all designated States except US)*: **NEW YORK UNIVERSITY** [US/US]; 70 Washington Square South, New York, NY 10012-1091 (US).

(72) **Inventors; and**
(75) **Inventors/Applicants** *(for US only)*: **JENSON, Jens** [US/US]; 348 Central Park Avenue, Apt. C-15, Scarsdale, NY 10583 (US). **HELPERN, Joseph, A.** [US/US]; 51 Angola Road, Cornwall, NY 12518 (US).

(74) **Agents**: **ABELEV, Gary** et al.; DORSEY & WHITNEY LLP, 250 Park Avenue, New York, NY 10177 (US).

(81) **Designated States** *(unless otherwise indicated, for every kind of national protection available)*: AE, AG, AL, AM, AO, AT, AU, AZ, BA, BB, BG, BH, BR, BW, BY, BZ, CA, CH, CL, CN, CO, CR, CU, CZ, DE, DK, DM, DO, DZ, EC, EE, EG, ES, FI, GB, GD, GE, GH, GM, GT, HN, HR, HU, ID, IL, IN, IS, JP, KE, KG, KM, KN, KP, KR, KZ, LA, LC, LK, LR, LS, LT, LU, LY, MA, MD, ME, MG, MK, MN, MW, MX, MY, MZ, NA, NG, NI, NO, NZ, OM, PE, PG, PH, PL, PT, RO, RS, RU, SC, SD, SE, SG, SK, SL, SM, ST, SV, SY, TJ, TM, TN, TR, TT, TZ, UA, UG, US, UZ, VC, VN, ZA, ZM, ZW.

(84) **Designated States** *(unless otherwise indicated, for every kind of regional protection available)*: ARIPO (BW, GH, GM, KE, LS, MW, MZ, NA, SD, SL, SZ, TZ, UG, ZM, ZW), Eurasian (AM, AZ, BY, KG, KZ, MD, RU, TJ, TM), European (AT, BE, BG, CH, CY, CZ, DE, DK, EE,

[Continued on next page]

(54) **Title**: SYSTEM, METHOD AND COMPUTER ACCESSIBLE MEDIUM FOR PROVIDING REAL-TIME DIFFUSIONAL KURTOSIS IMAGING

(57) **Abstract**: An exemplary method, system, and computer- accessible medium can be provided for determining a measure of diffusional kurtosis by receiving data relating to at least one diffusion weighted image, and determining a measure of a diffusional kurtosis as a function of the received data using a closed form solution procedure.

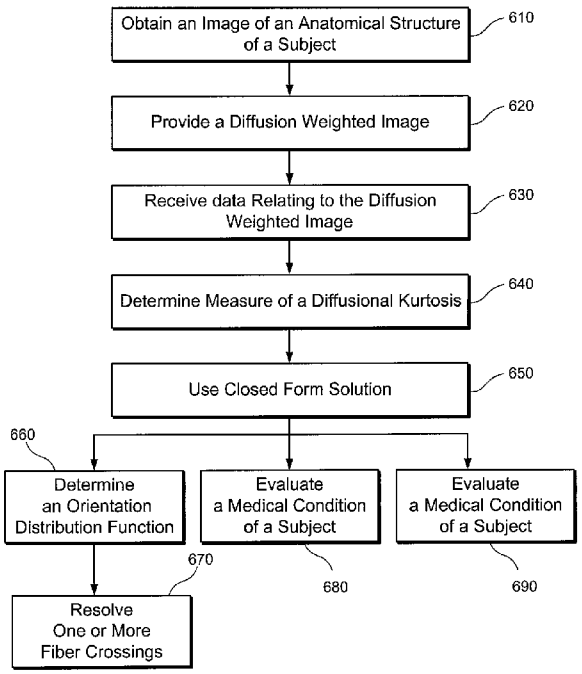

F I G. 9

WO 2010/017524 A2

ES, FI, FR, GB, GR, HR, HU, IE, IS, IT, LT, LU, LV, MC, MK, MT, NL, NO, PL, PT, RO, SE, SI, SK, SM, TR), OAPI (BF, BJ, CF, CG, CI, CM, GA, GN, GQ, GW, ML, MR, NE, SN, TD, TG).

Published:

— *without international search report and to be republished upon receipt of that report (Rule 48.2(g))*

SYSTEM, METHOD AND COMPUTER ACCESSIBLE MEDIUM FOR PROVIDING REAL-TIME DIFFUSIONAL KURTOSIS IMAGING

CROSS-REFERENCE TO RELATED APPLICATIONS

[0001] This application relates to and claims priority from United States Patent Application Serial No. 61/087,111 filed August 7, 2008, the entire disclosure of which is hereby incorporated herein by reference.

FIELD OF THE DISCLOSURE

[0002] The present disclosure relates to exemplary embodiments of systems, methods and computer-accessible mediums for providing real-time diffusional kurtosis imaging.

BACKGROUND INFORMATION

[0003] Diffusion anisotropy of water in biological tissues is conventionally quantified with the diffusion tensor (DT) and related indices such as the fractional anisotropy. DT describes the diffusion displacement probability using a Gaussian distribution function. One of the main applications of the DT is tracing the white matter pathways in the brain using local estimates of the fiber orientations. However, in regions with complex fiber configurations, DT likely fails to describe the full directional information of the diffusion process. Most notably, the DT is not able to resolve fiber crossing, which occurs in many brain regions. A more complete depiction of the water diffusion displacement is given by the probability density function (PDF). PDF can be approximated using q-space imaging techniques, but these techniques require diffusion measurements for a large range of diffusion weightings and diffusion directions. To overcome these limitations, an orientation distribution function (ODF) has been provided for diffusion displacement probability distribution.

[0004] Several approaches have been proposed to estimate the ODF. One such approach is the q-ball imaging (QBI), which is based on a Funk transform of high angular resolution diffusion imaging (HARDI) data. The QBI approach has been extended to explore the spherical harmonic basis functions and multiple wavevector fusion. For brain imaging, each of these techniques has several limitations including the need for high b values (i.e., 3000 s/mm^2 or above) and a large number of encoding directions or the assumption of specific diffusion properties for the investigated fiber populations.

[0005] Diffusional kurtosis is a quantitative measure of the degree to which the diffusion displacement probability distribution deviates from a Gaussian form. Diffusional Kurtosis Imaging (DKI) is a magnetic resonance imaging (MRI) technique for measuring this quantity. However, conventional DKI methods require substantial time (approximately 1 hour or more) for post-processing of the acquired images which may be a significant disadvantage in clinical practice.

[0006] Thus, it can be desirable to provide exemplary embodiments of method, system and computer accessible medium for providing real-time diffusional kurtosis imaging, and to estimate the orientation distribution function, which can reduce or avoid at least some of the problems encountered by the conventional techniques as set out above.

SUMMARY OF EXEMPLARY EMBODIMENTS OF DISCLOSURE

[0007] At least some of the above described problems can be addressed by exemplary embodiments of the system, method and computer accessible medium according to the present disclosure. For example, using such exemplary embodiments, it is possible to provide a method for determining a measure of diffusional kurtosis, which comprises receiving data relating to at least one diffusion weighted image, and using a computer

arrangement, determining a measure of a diffusional kurtosis as a function of the received data using a closed form solution procedure. The method can further comprise performing (i) providing the measure of the diffusional kurtosis to a display device, and/or (ii) recording the measure of the diffusional kurtosis. At least one diffusion weighted image can be acquired for three or more b-values. Such one or more diffusion weighted images can be acquired for 15 or more gradient directions.

[0008] The measure of the diffusional kurtosis can be determined using a mean kurtosis procedure. The mean kurtosis can be determined by averaging measures of a diffusion and a kurtosis over each gradient direction. The closed form solution procedure can include at least one or more elliptic integrals, and such one or more elliptic integrals can be associated with eigenvalues of at least one diffusion tensor based on the at least one diffusion weighted image. Such one or more elliptic integrals can be associated with at least one Carlson symmetric form of an elliptic integral.

[0009] The measure of the diffusional kurtosis can be an axial kurtosis and/or a radial kurtosis. At least a portion of the received data can relate to at least one orientation distribution function, the portion of the received data being calculated using the measure of the diffusional kurtosis. The exemplary method can further comprise resolving at least one fiber crossing using the received data from the at least one orientation distribution function. Such one or more fibers crossing can be a crossing of at least one of two fibers, three fibers or four fibers.

[0010] The exemplary method can further comprise providing a directional color map of the at least one fiber crossing, whereas the directional color map can provide fiber direction estimates as a function of the data associated with the orientation distribution

function(s). A fiber tractography can be performed using the data associated with the orientation distribution function(s).

[0011] The method can further comprise analyzing white matter connectivity patterns using the data associated with the at least one orientation distribution function, and estimating white matter pathways using the data associated with the at least one orientation distribution function. The exemplary method can further comprise analyzing fibers tracts which at least one of cross, kiss, branch, merge or splay, using the data associated with the orientation distribution function(s).

[0012] The received data associated with the orientation distribution function(s) can include Gaussian diffusion contributions and substantially exclude non-Gaussian diffusion contributions, include non-Gaussian diffusion contributions and substantially exclude Gaussian diffusion contributions or include Gaussian diffusion contributions and non-Gaussian diffusion contributions.

[0013] The data associated with the orientation distribution function(s) can be an approximation of an integral of a function depending on diffusion and kurtosis coefficients over a perpendicularly-oriented great circle.

[0014] The method can further comprise assessing at least one medical condition of a subject using the measure of the diffusional kurtosis. The medical condition(s) can be a neurological disease and/or a neuro-degenerative diseases. The medical condition(s) can be Alzheimer's disease, stroke, head trauma, attention deficit hyperactivity disorder and/or schizophrenia. The at least one medical condition can be assessed by comparing further data relating to the subject with predetermined control data, and the control data can comprise age-matched control data.

[0015] The method can further comprise determining a measure of a diffusional restrictivity using the measure of the diffusional kurtosis. The measure of the diffusional restrictivity can be determined from a diffusion tensor and a kurtosis tensor relating to the diffusion weighted image(s). The measure of the diffusional restrictivity can include a measure of Gaussian restrictivity which substantially excludes non-Gaussian restrictivity, include a measure of non-Gaussian restrictivity which substantially excludes Gaussian restrictivity, or include a measure of Gaussian restrictivity and non-Gaussian restrictivity.

[0016] The measure of diffusional restrictivity can be determined using a first measure dependent on diffusivity and a second measure dependent on diffusional kurtosis. The second measure can reflect non-Gaussian diffusion contributions to a diffusion signal.

[0017] The exemplary method can further comprise identifying at least one region of interest in an anatomical structure based on the measure of the diffusional kurtosis and/or the measure of the diffusional restrictivity. The anatomical structure can comprise a brain tissue. The at least one region of interest can indicate differences in microstructure between different portions of the anatomical structure. The at least one region of interest can at least partially distinguish between a reversibly injured tissue and an irreversibly injured tissue.

[0018] Using such exemplary embodiments, it is also possible to provide a system for determining a measure of diffusional kurtosis comprising a first arrangement configured to receive data relating to at least one diffusion weighted image, and a second arrangement configured to determine a measure of a diffusional kurtosis as a function of the received data using a closed form solution procedure. The second arrangement can be further configured to perform (i) provide the measure of the diffusional kurtosis to a display device, and/or (ii) record the measure of the diffusional kurtosis. The diffusion

weighted image(s) can be acquired for three or more b-values, and the diffusion weighted image(s) can be acquired for 15 or more gradient directions.

[0019] The second arrangement can be further configured to assess at least one medical condition of a subject using the measure of the diffusional kurtosis, and can be further configured to determine a measure of a diffusional restrictivity using the measure of the diffusional kurtosis. The second arrangement can be further configured to identify at least one region of interest in an anatomical structure based on the measure of the diffusional kurtosis and/or the measure of the diffusional restrictivity.

[0020] Using such exemplary embodiments, it is also possible to provide a computer-accessible medium for determining a measure of diffusional kurtosis, the computer-accessible medium including instructions thereon, wherein, when a computing arrangement executes the instructions, the computing arrangement is configured to perform procedures comprising receiving data relating to at least one diffusion weighted image, and determining a measure of a diffusional kurtosis as a function of the received data using a closed form solution procedure. The computing arrangement can be further configured to (i) provide the measure of the diffusional kurtosis to a display device, and/or (ii) record the measure of the diffusional kurtosis.

[0021] These and other objects, features and advantages of the present disclosure will become apparent upon reading the following detailed description of embodiments of the present disclosure, when taken in conjunction with the appended claims.

BRIEF DESCRIPTION OF THE DRAWINGS

[0022] The foregoing and other exemplary objects of the present disclosure will be apparent upon consideration of the following detailed description, taken in conjunction

with the accompanying exemplary drawings and claims, in which like reference characters refer to like parts throughout, and in which:

[0023] Figs. 1(a)-1(f) are illustrations of exemplary three dimensional surfaces of exact and estimated ODF's for exemplary diffusion models;

[0024] Figs. 2(a)-2(f) are other illustrations of further exemplary three dimensional surfaces of exact and estimated ODF's for the exemplary diffusion models;

[0025] Figs. 3(a)-3(e) are illustrations of exemplary ODF maps of the brainstem;

[0026] Figs. 4(a)-4(e) are other illustrations of further exemplary ODF maps of the brainstem;

[0027] Fig. 5(a)-5(e) are is illustrations of the exemplary ODF maps of the intersection between the posterior region of the superior longitudinal fasciculus with the projection fibers of the corona radiata and the posterior transverse association fibers;

[0028] Figs. 6(a)-6(d) are illustrations of exemplary brain images of a mean diffusivity, axial diffusivity, radial diffusivity and a fractional anisotropy, respectively, provided by conventional diffusion tensor imaging;

[0029] Figs. 7(a)-7(c) are illustrations of exemplary parametric maps derived with real-time diffusional kurtosis imaging obtained using exemplary embodiments of the present disclosure;

[0030] Fig. 8 is a flow diagram according to an exemplary embodiment of a method of an exemplary real-time diffusional kurtosis imaging;

[0031] Fig. 9 is a flow diagram according to an exemplary embodiment of a method of the present disclosure; and

[0032] Fig. 10 is a block diagram of an exemplary embodiment of a system according to the present disclosure.

[0033] Throughout the figures, the same reference numerals and characters, unless otherwise stated, are used to denote like features, elements, components or portions of the illustrated embodiments. Moreover, while the subject invention will now be described in detail with reference to the figures, it is done so in connection with the illustrative embodiments. It is intended that changes and modifications can be made to the described embodiments without departing from the true scope and spirit of the subject disclosure.

DETAILED DESCRIPTION OF EXEMPLARY EMBODIMENTS OF DISCLOSURE

[0034] Exemplary embodiments of the methodologies and procedures according to the present disclosure which can be implemented by the exemplary embodiments of system, method and computer-accessible medium according to the present disclosure will now be described, at least to some extent, with reference to the figures.

[0035] Diffusional Kurtosis Imaging (DKI) is an exemplary magnetic resonance imaging technique, which can be useful for the assessment of a variety of diseases including stroke, Alzheimer's disease, head trauma, schizophrenia and attention deficit hyperactivity disorder. In evaluating acute stroke processed DKI, results should ideally be available on-line within seconds after the scanning so that timely treatment decisions can be made. Real-time DKI analysis routinely available on commercial Magnetic Resonance Imaging (MRI) scanners would also greatly facilitate the application and

increase the usefulness of DKI for many other diseases. "Real-time" can comprise but is not limited to, e.g., an analysis in which results, measurements, etc. are obtained within approximately one minute, and sometimes within approximately 30 seconds.

[0036] In the exemplary embodiments of the present disclosure, real-time DKI method, system and computer-accessible medium can be provided, which can be based both on a particular data acquisition scheme and on a mathematical prescription for rapid analysis of the images.

Exemplary Data Acquisition Procedure(s)

[0037] An exemplary DKI data set utilizes that diffusion-weighted (DW) images can be acquired for approximately 3 or more b-values and approximately 15 or more gradient directions. A b-value is a factor of diffusion weighted sequences, and summarizes the influence of the gradients on diffusion weighted images. The higher the b-value, the stronger the diffusion weighting. Particularly, there can be an advantage in using precisely 3 b-values in that this can allow one to avoid numerical nonlinear fitting procedures which are both time-consuming and often suffer from convergence problems. In this exemplary manner, the post-processing time can be significantly reduced. An exemplary choice of b-values for brain imaging can be b = 0, 1000, 2000 (s/mm^2), but the exemplary embodiments of the present disclosure is not restricted to these exemplary values. The gradient directions can typically be distributed uniformly on a sphere. An exemplary selection can be a set of 30 directions defined by a truncated icosahedron. For each exemplary b-value and direction, one or more images may be acquired. If more than one image is acquired, such exemplary images can be co-registered and averaged prior to data processing.

Exemplary Data Processing Procedure(s)

[0038] A first procedure in the exemplary data processing methodology can be to determine the diffusion coefficient (D_i) and diffusional kurtosis (K_i) for the ith gradient direction in each voxel. Voxels can be processed independently according to the same or similar procedure, and so it can be sufficient to describe the procedure for a single voxel. An exemplary closed form solution can be used to determine a measure of diffusional kurtosis, as will be set out below. An equation or system of equations can have a closed-form solution, e.g., when at least one solution can be expressed as a closed-form expression. A closed-form expression can, e.g., be expressed analytically in terms of a bounded number of certain functions.

[0039] If the DW signal intensity corresponds to an ith direction for a given voxel and a b-value is indicated by $S_i(b)$, then:

$$D_i = \frac{(b_3 + b_1)D_i^{(12)} - (b_2 + b_1)D_i^{(13)}}{b_3 - b_2} \qquad [1]$$

$$K_i = 6\frac{D_i^{(12)} - D_i^{(13)}}{(b_3 - b_2)D_i^2} \qquad [2]$$

[0040] where

$$D_i^{(12)} \equiv \frac{\ln\left[\frac{S_i(b_1)}{S_i(b_2)}\right]}{b_2 - b_1}, \qquad D_i^{(13)} \equiv \frac{\ln\left[\frac{S_i(b_1)}{S_i(b_3)}\right]}{b_3 - b_1}, \qquad [3]$$

and b_1, b_2, b_3 represent the three b-values used for data acquisition.

[0041] In one exemplary procedure, from the set of D_i and K_i, the diffusion tensor and the diffusional kurtosis tensor can be constructed by linear inversion. The exemplary linear system for the diffusion tensor can be represented by:

$$\begin{pmatrix} D_1 \\ D_2 \\ \vdots \\ D_N \end{pmatrix} = \begin{pmatrix} \left[g_1^{(1)}\right]^2 & \left[g_2^{(1)}\right]^2 & \left[g_3^{(1)}\right]^2 & 2g_1^{(1)}g_2^{(1)} & 2g_1^{(1)}g_3^{(1)} & 2g_2^{(1)}g_3^{(1)} \\ \left[g_1^{(2)}\right]^2 & \left[g_2^{(2)}\right]^2 & \left[g_3^{(2)}\right]^2 & 2g_1^{(2)}g_2^{(2)} & 2g_1^{(2)}g_3^{(2)} & 2g_2^{(2)}g_3^{(2)} \\ \vdots & \vdots & \vdots & \vdots & \vdots & \vdots \\ \left[g_1^{(N)}\right]^2 & \left[g_2^{(N)}\right]^2 & \left[g_3^{(N)}\right]^2 & 2g_1^{(N)}g_2^{(N)} & 2g_1^{(N)}g_3^{(N)} & 2g_2^{(N)}g_3^{(N)} \end{pmatrix} \begin{pmatrix} D_{11} \\ D_{22} \\ D_{33} \\ D_{12} \\ D_{13} \\ D_{23} \end{pmatrix} \quad [4]$$

[0042] where N can be the number of gradient directions, $g_i^{(n)}$ can be the ith component of the nth gradient direction vector ($|\mathbf{g}| = 1$), and D_{ij} can be the components of the diffusion tensor. The linear system for the diffusional kurtosis tensor can then be represented by:

$$\begin{pmatrix} D_1^2K_1 \\ D_2^2K_2 \\ \vdots \\ D_N^2K_N \end{pmatrix} = \overline{D}^2 \begin{pmatrix} \left[g_1^{(1)}\right]^4 & \cdots & 4\left[g_1^{(1)}\right]^3 g_2^{(1)} & \cdots & 6\left[g_1^{(1)}\right]^2\left[g_2^{(1)}\right]^2 & \cdots & 12g_1^{(1)}g_2^{(1)}\left[g_3^{(1)}\right]^2 \\ \left[g_1^{(2)}\right]^4 & \cdots & 4\left[g_1^{(2)}\right]^3 g_2^{(2)} & \cdots & 6\left[g_1^{(2)}\right]^2\left[g_2^{(2)}\right]^2 & \cdots & 12g_1^{(2)}g_2^{(2)}\left[g_3^{(2)}\right]^2 \\ \vdots & \vdots & \vdots & \vdots & \vdots & \vdots & \vdots \\ \left[g_1^{(N)}\right]^4 & \cdots & 4\left[g_1^{(N)}\right]^3 g_2^{(N)} & \cdots & 6\left[g_1^{(N)}\right]^2\left[g_2^{(N)}\right]^2 & \cdots & 12g_1^{(N)}g_2^{(N)}\left[g_3^{(N)}\right]^2 \end{pmatrix} \begin{pmatrix} W_{1111} \\ W_{2222} \\ W_{3333} \\ W_{1112} \\ W_{1113} \\ W_{1222} \\ W_{1333} \\ W_{2223} \\ W_{1122} \\ W_{1133} \\ W_{2233} \\ W_{2333} \\ W_{1123} \\ W_{1223} \\ W_{1233} \end{pmatrix}, \quad [5]$$

where W_{ijkl} can be the components of the diffusional kurtosis tensor and $\overline{D}$ can be the mean diffusivity (MD) which may be calculated from

$$\overline{D} = \frac{1}{3}\left(D_{11} + D_{22} + D_{33}\right) \qquad [6]$$

[0043] Both D_{ij} and W_{ijkl} can be symmetric with respect to permutation of their indices so that these tensors are determined by the components appearing in Eqs. [4] and [5]. These two exemplary linear systems can be readily solved by an exemplary method which can utilize a singular value decomposition. Since the matrices for the two exemplary linear systems can depend on the gradient directions, their singular value decompositions can be calculated once for any particular choice of directions. Accordingly, this exemplary procedure in the data processing would require minimal computational time.

[0044] For additional exemplary processing, it can be convenient to rotate to a reference frame (the eigenframe) in which the diffusion tensor is diagonal. In the eigenframe, the diffusion tensor can takes the form of:

$$\widetilde{D}_{ij} = \lambda_i \delta_{ij}, \qquad [7]$$

where λ_i can be the eigenvalues and δ_{ij} can be the kronecker delta, and the diffusional kurtosis tensor can take the form of:

$$\widetilde{W}_{ijkl} = \sum_{i',j',k',l'} R_{ii'} R_{jj'} R_{kk'} R_{ll'} W_{i'j'k'l'} \qquad [8]$$

with R_{ij} being the rotation matrix and the sums being carried out from Eqs. 1 to 3 provided herein. The exemplary rotation matrix can be given by:

$$R_{ij} = u_j^{(i)} \qquad [9]$$

where $u_j^{(i)}$ can be the jth component of the ith eigenvector for D_{ij}. The eigenvalues and eigenvectors can be determined by using any of several exemplary standard techniques, such as Jacobi's method. Without loss of generality, it is possible to order the eigenvalues so that ($\lambda_1 \le \lambda_2 \le \lambda_3$).

[0045] From the diffusion tensor eigenvalues, the axial diffusivity can be obtained by:

$$D_{\|} = \lambda_3 , \qquad [10]$$

and the radial diffusivity:

$$D_{\perp} = \frac{1}{2}(\lambda_1 + \lambda_2). \qquad [11]$$

[0046] It is also possible to determine the fractional anisotropy (FA) as follows:

$$FA = \sqrt{\frac{(\lambda_1 - \lambda_2)^2 + (\lambda_1 - \lambda_3)^2 + (\lambda_2 - \lambda_3)^2}{2(\lambda_1^2 + \lambda_2^2 + \lambda_3^2)}} \qquad [12]$$

[0047] From the eigenframe representation of the diffusional kurtosis tensor, the mean kurtosis (MK) can be calculated as follows:

$$\begin{aligned} \overline{K} = {} & 6A_{1122}(\lambda_1, \lambda_2, \lambda_3)\tilde{W}_{1122} + 6A_{1122}(\lambda_1, \lambda_3, \lambda_2)\tilde{W}_{1133} + 6A_{1122}(\lambda_2, \lambda_3, \lambda_1)\tilde{W}_{2233} \\ & + A_{3333}(\lambda_2, \lambda_3, \lambda_1)\tilde{W}_{1111} + A_{3333}(\lambda_1, \lambda_3, \lambda_2)\tilde{W}_{2222} + A_{3333}(\lambda_1, \lambda_2, \lambda_3)\tilde{W}_{3333}, \end{aligned} \qquad [13]$$

where

$$A_{1122}(\lambda_1, \lambda_2, \lambda_3) = \frac{(\lambda_1 + \lambda_2 + \lambda_3)^2}{18(\lambda_1 - \lambda_2)^2}\left[\frac{\lambda_1 + \lambda_2}{\sqrt{\lambda_1 \lambda_2}} R_F\left(\frac{\lambda_3}{\lambda_1}, \frac{\lambda_3}{\lambda_2}, 1\right) + \frac{2\lambda_3 - \lambda_1 - \lambda_2}{3\sqrt{\lambda_1 \lambda_2}} R_D\left(\frac{\lambda_3}{\lambda_1}, \frac{\lambda_3}{\lambda_2}, 1\right) - 2\right] \qquad [14]$$

and

$$A_{3333}(\lambda_1,\lambda_2,\lambda_3)= \frac{(\lambda_1+\lambda_2+\lambda_3)^2}{18(\lambda_3-\lambda_1)(\lambda_3-\lambda_2)}\left[\frac{\sqrt{\lambda_1\lambda_2}}{\lambda_3}R_F\left(\frac{\lambda_3}{\lambda_1},\frac{\lambda_3}{\lambda_2},1\right)+\frac{3\lambda_3^2-\lambda_1\lambda_2-\lambda_1\lambda_3-\lambda_2\lambda_3}{3\lambda_3\sqrt{\lambda_1\lambda_2}}R_D\left(\frac{\lambda_3}{\lambda_1},\frac{\lambda_3}{\lambda_2},1\right)-1\right].$$

[15]

with R_F and R_D being Carlson's elliptic integrals. Since there are highly efficient numerical algorithms for calculating Carlson's elliptic integrals, Eqs. [14] and [15] facilitate fast determination of the MK.

[0048] When $\lambda_1=\lambda_2$, Eq. [14] has a removable singularity. This can be resolved with:

$$A_{1122}(\lambda_1,\lambda_1,\lambda_3)=\frac{(2\lambda_1+\lambda_3)^2}{144\lambda_1^2(\lambda_3-\lambda_1)^2}\left[\lambda_1(2\lambda_1+\lambda_3)+\lambda_3(\lambda_3-4\lambda_1)\alpha\left(1-\frac{\lambda_3}{\lambda_1}\right)\right] \quad [16]$$

where

$$\alpha(x)\equiv\begin{cases}\dfrac{1}{\sqrt{x}}\operatorname{arctanh}(\sqrt{x}), & \text{if } x>0,\\ \dfrac{1}{\sqrt{-x}}\arctan(\sqrt{-x}), & \text{if } x<0.\end{cases} \quad [17]$$

[0049] When $\lambda_1=\lambda_3$ or $\lambda_2=\lambda_3$, Eq. [15] has a removable singularity, which can be resolved with:

$$A_{3333}(\lambda_1,\lambda_2,\lambda_1)=3A_{1122}(\lambda_1,\lambda_1,\lambda_2);\ A_{3333}(\lambda_1,\lambda_2,\lambda_2)=3A_{1122}(\lambda_2,\lambda_2,\lambda_1). \quad [18]$$

[0050] Further, for the special case when $\lambda_1=\lambda_2=\lambda_3$:

$$A_{1122}=\frac{1}{15};\qquad A_{3333}=\frac{1}{5}. \quad [19]$$

[0051] Similarly, it is possible to determine the axial kurtosis from:

$$K_{\parallel} = \frac{(\lambda_1 + \lambda_2 + \lambda_3)^2}{9\lambda_3^2} \tilde{W}_{3333}, \quad [20]$$

and the radial kurtosis from:

$$K_{\perp} = 6C_{1122}(\lambda_1, \lambda_2, \lambda_3)\tilde{W}_{1122} + C_{1111}(\lambda_1, \lambda_2, \lambda_3)\tilde{W}_{1111} + C_{1111}(\lambda_2, \lambda_1, \lambda_3)\tilde{W}_{2222}, \quad [21]$$

where

$$C_{1111}(\lambda_1, \lambda_2, \lambda_3) = \frac{(\lambda_1 + \lambda_2 + \lambda_3)^2}{18\lambda_1(\lambda_1 - \lambda_2)^2}\left(2\lambda_1 + \frac{\lambda_2^2 - 3\lambda_1\lambda_2}{\sqrt{\lambda_1\lambda_2}}\right), \quad [22]$$

and

$$C_{1122}(\lambda_1, \lambda_2, \lambda_3) = \frac{(\lambda_1 + \lambda_2 + \lambda_3)^2}{18(\lambda_1 - \lambda_2)^2}\left(\frac{\lambda_1 + \lambda_2}{\sqrt{\lambda_1\lambda_2}} - 2\right). \quad [23]$$

[0052] For the special case of $\lambda_1 = \lambda_2$, these determinations can reduce to:

$$C_{1111}(\lambda_1, \lambda_1, \lambda_3) = \frac{(2\lambda_1 + \lambda_3)^2}{24\lambda_1^2}, \quad [24]$$

and

$$C_{1122}(\lambda_1, \lambda_1, \lambda_3) = \frac{(2\lambda_1 + \lambda_3)^2}{72\lambda_1^2}. \quad [25]$$

[0053] Eqs. [10] - [12] can be standard results used in diffusional tensor imaging data processing. However, Eqs. [13] - [25] can be important for real-time DKI data processing.

Exemplary Orientation Distribution Function(s)

[0054] One exemplary advantage of the orientation distribution function (ODF) for diffusion displacement probability distribution is that it can resolve fiber crossings in a model independent manner. A mathematical relationship between the ODF and the DK can demonstrate the ability of the DK-ODF to resolve fiber crossings by using simulations. In addition, an exemplary application of the DK-ODF to the brain is provided by exemplary examples of DK-ODF's calculated from human imaging data.

Exemplary Diffusional Kurtosis Approximation of Orientation Distribution Function(s)

[0055] Exemplary diffusional kurtosis imaging procedures can extend the Gaussian approximation of the diffusion distribution function by considering non-Gaussian contributions through an additional kurtosis term. For a direction specified by the unit vector n , the diffusion signal can be written as:

$$\ln[S(b)] - \ln[S(0)] = -b\sum_{i=1}^{3}\sum_{j=1}^{3} n_i n_j D_{ij} + \frac{1}{6}b^2\bar{D}^2\sum_{i=1}^{3}\sum_{j=1}^{3}\sum_{k=1}^{3}\sum_{l=1}^{3} n_i n_j n_k n_l W_{ijkl} \qquad [26]$$

where D_{ij} are the elements of the second order diffusion tensor D, and W_{ijkl} the elements of the forth order kurtosis tensor W. D can represent the mean diffusivity $D \equiv \text{Trace}(D)/3$. The exemplary diffusion and kurtosis coefficients along the n direction can be related to the respective tensors by the following equations:

$$D(\hat{\mathbf{n}}) = \hat{\mathbf{n}}^T \cdot \mathbf{D} \cdot \hat{\mathbf{n}} = \sum_{i=1}^{3}\sum_{j=1}^{3} \hat{n}_i \hat{n}_j D_{ij}$$

$$K(\hat{\mathbf{n}}) = \frac{\bar{D}^2}{D(\hat{\mathbf{n}})^2} \cdot \sum_{i=1}^{3}\sum_{j=1}^{3}\sum_{k=1}^{3}\sum_{l=1}^{3} \hat{n}_i \hat{n}_j \hat{n}_k \hat{n}_l W_{ijkl} \qquad [27a, 27b]$$

[0056] Both D_{ij} and W_{ijkl}, can be symmetric with respect to an interchange of indices; consequently, D can have 6 independent degrees of freedom, and W can have 15 independent degrees of freedom. Eq. [26] can be rewritten in terms of D(n) and K(n) as:

$$\ln[S(b)] = \ln[S(0)] - bD(\hat{\mathbf{n}}) + \frac{1}{6}b^2 D(\hat{\mathbf{n}})^2 K(\hat{\mathbf{n}}) \qquad [28]$$

[0057] If P(*s, t*) represents the water diffusion displacement probability distribution for a displacement s and a diffusion time t, the ODF can be defined as its radial projection:

$$\psi(\hat{\mathbf{n}}) = \frac{1}{Z}\int_0^\infty ds\, P(s\hat{\mathbf{n}}, t) \qquad [29]$$

where Z is a normalization constant. An exemplary result of the DK-ODF approximation can be provided by:

$$\psi(\hat{\mathbf{n}}) \approx \psi_{DK}(\hat{\mathbf{n}}) \equiv \frac{1}{48\pi^2 Zt}\int d^3u \frac{3 + K(\mathbf{u})}{D(\mathbf{u})} \cdot \delta(\hat{\mathbf{n}} \cdot \mathbf{u}) \cdot \delta(|\mathbf{u}| - 1), \qquad [30]$$

with δ indicating the Dirac delta function. Because of the exemplary delta functions, the exemplary integral in Eq. [30] can be one-dimensional and corresponds to a Funk transform, which can reduce the determination of the ODF value along a direction n to an integration of the signal values on a perpendicularly oriented great circle. When n coincides with a coordinate axis 1, Eq. [30] takes the form:

$$\psi(\hat{\mathbf{z}}) \approx \psi_{DK}(\hat{\mathbf{z}}) = \frac{1}{48\pi^2 Zt}\int_0^{2\pi} d\varphi \frac{3 + K(\theta, \varphi)}{D(\theta, \varphi)}\bigg|_{\theta=\pi/2}, \qquad [31]$$

where θ is the polar angle and φ is the azimuthal angle with respect to **z**. Thus, an exemplary approximation for the ODF in a particular direction can be obtained by integrating a function depending on the diffusion and kurtosis coefficients over the perpendicularly oriented great circle. The exemplary DK-ODF can facilitate the resolution of fiber crossings. Since a standard DKI data set can provide estimates for both the diffusion tensor and the kurtosis tensor, it is possible to use Eq. [31] to also determine an approximate ODF. For example, $D(\theta, \varphi)$ and $K(\theta, \varphi)$ under the integrand can be approximated at any location on the great circle from the diffusion and kurtosis tensors using Eqs. [27a] and [27b].

[0058] In the DK approximation (e,g,m Eq. [31]), the ODF can be represented as a sum of two terms as follows:

$$\psi(\hat{\mathbf{z}}) \approx \psi_{DK}(\hat{\mathbf{z}}) = \frac{1}{48\pi^2 Zt}\int_0^{2\pi} d\varphi \frac{3}{D(\theta,\varphi)}\bigg|_{\theta=\pi/2} + \frac{1}{48\pi^2 Zt}\int_0^{2\pi} d\varphi \frac{K(\theta,\varphi)}{D(\theta,\varphi)}\bigg|_{\theta=\pi/2} \qquad [32]$$

where the first term corresponds to the Gaussian diffusion contributions and the second to the non-Gaussian diffusion contributions. These exemplary diffusion contribution can be referred to as the Gaussian and non-Gaussian (NG) DK estimated ODFs, respectively. The total ODF can then be written as:

$$\psi_{DK}(\hat{\mathbf{n}}) = \psi_{G\text{-}DK}(\hat{\mathbf{n}}) + \psi_{NG\text{-}DK}(\hat{\mathbf{n}}) \qquad [33]$$

Exemplary ODF for Gaussian Diffusion Approximation Procedure(s)

[0059] For Gaussian diffusion, the displacement probability distribution can have the form of:

$$P(\mathbf{s},t) = \frac{1}{(4\pi t)^{3/2}|\mathbf{D}|^{1/2}} \cdot \exp\left[-\mathbf{s}^T \cdot \mathbf{D}^{-1} \cdot \mathbf{s}/4t\right] \qquad [34]$$

[0060] For this exemplary embodiment, it can be verified that K = 0 and that:

$$\psi(\hat{\mathbf{n}}) = \psi_{DT}(\hat{\mathbf{n}}) \equiv \frac{1}{8\pi Zt|\mathbf{D}|^{1/2}} \cdot \left(\frac{1}{\hat{\mathbf{n}}^T \cdot \mathbf{D}^{-1} \cdot \hat{\mathbf{n}}}\right)^{3/2} \qquad [35]$$

[0061] An exemplary disadvantage of the DT-ODF is that it may not allow fiber crossings to be resolved.

[0062] More generally, ψ_{DT} can be regarded as a "diffusion tensor approximation" for the ODF. Equation [35] can be used to fix the normalizations of the ODF approximations by setting:

$$Z = \frac{1}{8\pi \bar{D} t} \qquad [36]$$

so that the ODF is dimensionless and equal to unity for isotropic Gaussian diffusion.

Exemplary Simulations

[0063] To test the DK-ODF, a multi-compartment model can be utilized with the displacement probability distributions of the form of:

$$P(\mathbf{s},t) = \sum_{m=1}^{N} f_m \frac{1}{(4\pi t)^{3/2}|\mathbf{D}^{(m)}|^{1/2}} \cdot \exp\left\{-\mathbf{s}^T \cdot \left[\mathbf{D}^{(m)}\right]^{-1} \cdot \mathbf{s}/4t\right\}, \qquad [37]$$

where N is the number of compartments, $D^{(m)}$ the diffusion tensor for the mth compartment, and f_m its corresponding water fraction with the water fractions f_m adding to unity $\sum_{m=1}^{N} f_m = 1$.

[0064] For example, the exact ODF for this model can be given by:

$$\psi(\hat{\mathbf{n}}) = \sum_{m=1}^{N} \frac{f_m}{8\pi Z_l \left|\mathbf{D}^{(m)}\right|^{1/2}} \cdot \left\{ \frac{1}{\hat{\mathbf{n}}^T \cdot \left[\mathbf{D}^{(m)}\right]^{-1} \cdot \hat{\mathbf{n}}} \right\}^{3/2}. \qquad [38]$$

[0065] The exemplary diffusion and kurtosis tensors can be obtained as combinations of the diffusion tensors describing the individual compartments:

$$\mathbf{D} = \sum_{m=1}^{N} f_m \mathbf{D}^{(m)},$$

$$W_{ijkl} = \frac{1}{\bar{D}^2} \left\{ \sum_{m=1}^{N} f_m \left[D_{ij}^{(m)} D_{kl}^{(m)} + D_{ik}^{(m)} D_{jl}^{(m)} + D_{il}^{(m)} D_{jk}^{(m)} \right] - D_{ij} D_{kl} - D_{ik} D_{jl} - D_{il} D_{jk} \right\}. \qquad [39, 40]$$

[0066] The ODF-DK can be estimated using Eq. [32], where D(n) and K(n) values can be obtained from the diffusion and kurtosis tensor, respectively.

[0067] Exemplary mixed fiber models having two to four compartments were used. For all the models, the eigenvalues of $D^{(m)}$ were chosen to be 0.3, 0.3, and 1.8 $\mu m^2/ms$, so that the diffusion within each compartment was highly anisotropic (fractional anisotropy = 0.81). Mixtures with different weights were investigated. For each model, the exact and DK and QB estimated ODFs were calculated and displayed, as well as the exact and DK estimated non-Gaussian ODFs (NG-ODF). A b value of 4000s/mm^2 was assumed for

calculating the QB-ODF as an approximate and typical value. For comparison purposes, the Gaussian (DT) ODF was also calculated for each model.

[0068] Exemplary Diffusional Restrictivity

[0069] A diffusional restrictivity at a time t can is defined as:

$$R_D(t) = 2t\left\langle \frac{1}{[\mathbf{r}(t)-\mathbf{r}(0)]\cdot[\mathbf{r}(t)-\mathbf{r}(0)]} \right\rangle. \qquad [41]$$

[0070] where $\mathbf{r}(t)$ can be a diffusion path and the angle brackets indicate an averaging over a region of interest. The restrictivity may be calculated from the orientation distribution function using the equation:

$$R_D = 2Zt\int d^3u\, \psi(\mathbf{u})\delta(|\mathbf{u}|-1). \qquad [42]$$

[0071] From this, the approximate expression can be derived:

$$R_D \approx \frac{1}{12\pi}\int d^3u \frac{3+K(\mathbf{u})}{D(\mathbf{u})}\delta(|\mathbf{u}|-1). \qquad [43]$$

[0072] Since both $D(\mathbf{u})$ and $K(\mathbf{u})$ can be obtained with DKI, this shows how DKI can be used to estimate the diffusional restrictivity.

Exemplary MRI Experiment

[0073] Exemplary imaging experiments were conducted on a 3 T Trio MR system (Siemens Medical Solutions, Erlangen, Germany) using a body coil for transmission and an eight-element phase array coil for reception. Exemplary DKI data was obtained for six healthy volunteers using a predetermined protocol. Diffusion weighted images were acquired for 30 uniformly distributed gradient directions and for five b-values (500, 1000,

1500, 2000 and 2500 s/mm^2) using a twice refocused-spin-echo EPI sequence, which has been shown to significantly reduce the eddy-current-related distortions in the diffusion weighted images. In addition, data without any diffusion weighting (b=0 s/mm) was obtained. Other imaging parameters included: TR = 2000ms, TE = 109ms, FOV = 256x256mm^2, matrix = 128 x 128, a parallel imaging factor of 2, number of images averaged (NEX) = 2, 6/8 partial Fourier in phase-encoding direction, 15 axial slices, with a slice thickness of 2 (acquisition 1) or 4 mm (acquisition 2) and gap of 2 mm. The total duration for acquiring a DKI data set was 12 minutes.

Exemplary Image Data Processing Procedure(s)

[0074] The diffusion weighted images were first corrected for motion and spatially smoothed using SPM using a two-dimensional Gaussian filter with FWHM of 2.5 mm. The diffusion and kurtosis tensors were subsequently calculated. Only those data points that exceeded the value representing the 90th percentile of the noise range were included in the calculation, where noise values were sampled using a 10x10x13 volume situated outside a brain. The tensor calculation included: 1) estimation of the apparent diffusivity and kurtosis values along each of the thirty encoding directions using Levenberg–Marquardt nonlinear fitting algorithm for Eq. [28], 2) diffusion tensor estimation from a set of apparent diffusivities, and 3) kurtosis tensor estimation (using Eq. [27b]) using the apparent kurtosis values estimated at step (1) and the set of corrected apparent diffusion values obtained using the diffusion tensor estimated at step (2).

[0075] The exemplary diffusion tensor eigenvectors and eigenvalues, and the fractional anisotropy were calculated and used to obtain directional color maps and to depict the fiber direction estimates using a Gaussian approximation. The exemplary color maps were used for anatomical reference.

[0076] The non-Gaussian (NG), Gaussian, and total ODFs were calculated at each voxel using Eq. [32] on a grid of 60 x 60 data points (corresponding to equally spaced θ and φ values). For each grid point, the ODF value was estimated by integrating along the equator circle perpendicular to a grid point direction, and the D(n) and K(n) values in the integrand were obtained from the diffusion and kurtosis tensors, respectively. In order to better distinguish visually the directional variations in the ODF profile, a 0 to 1 resealed min-max version of the non-Gaussian ODF was also calculated (i.e., the minimum ODF value is scaled to 0 and the maximum ODF value is scaled to 1). The exemplary fiber directions at each voxel were determined from the ODF peaks. The ODF surfaces were superimposed onto mean kurtosis maps and were color-coded using the typical mapping of the x, y, and z spatial directions to a red, green, and blue color triad.

Further Exemplary Simulations

[0077] Figures 1(a) – 1(f) illustrate exemplary three-dimensional ODF surfaces for diffusion models including two (top row) and three (bottom row) equally contributing fibers (i.e., f_m=1/N) intersecting at a high angle (>80°). For example, Fig. 1(a) illustrates an exemplary exact ODF, Fig. 1(b) illustrates an exemplary DK estimation of the ODF, Fig. 1(c) illustrates an exemplary exact NG-ODF, Fig. 1(d) illustrates an exemplary DK estimation of the NG-ODF, Fig. 1(e) illustrates an exemplary q-ball estimation of the ODF (min-max scaled) for a b-value of 4000s/mm^2, and Fig. 1(f) illustrates an exemplary Gaussian estimation of the ODF. The directions of the exemplary component fibers are shown in these figures by the dashed lines, and the fiber orientations are (θ_1, φ_1) = (50°, 90°) and (θ_2, φ_2) = (130°, 90°) for N=2 and (θ_1, φ_1)= (60°, 90°), (θ_2, φ_2) = (120°, 40°), (03, 603) = (120°, 130°) for N=3. An appropriate correspondence can be seen between the direction of the fibers (indicated by dashed lines) and the ODF peaks for both the DK

and QB approximations, with no offset between the true and the estimated directions. The NG-ODF gives a good peak delineation.

[0078] In Figs. 2(a)-2(f), exemplary images of exemplary three dimensional surfaces of the exact and estimated ODF are illustrated for diffusion models with two fibers with volume fractions of 30% and 70% (top row) and two equally contributing fibers intersecting at an angle of 30° (bottom row). For example, Fig. 2(a) illustrates an exemplary exact ODF, Fig. 2(b) illustrates an exemplary DK estimation of the ODF, Fig. 2(c) illustrates an exemplary exact NG-ODF, Fig. 2(d) illustrates an exemplary DK estimation of the NG-ODF, Fig. 2(e) illustrates an exemplary q-ball estimation of the ODF (min-max scaled) for a b value of 4000 s/mm^2, and Fig. 2(f) illustrates an exemplary Gaussian estimation of the ODF. The directions of the exemplary component fibers are shown by dashed lines. The fiber orientations shown in Fig. 2(a) are the same as those in Fig. 1(a). The fiber orientations shown in Fig. 2(b) are: $(\theta 1, \varphi 1) = (50°, 90°)$ and $(\theta 2, \varphi 2) = (80°, 90°)$.

[0079] Individual fibers can be resolved in cases where one compartment has a greater contribution than the other one, as illustrated in Fig. 2(a). An appropriate approximation of the component fiber orientations can be observed for a small angle of intersection in Fig. 2(b), (angle of intersection = 30°) for the DK-ODF, though the ODF peaks were offset with respect to the chosen fiber direction by approximately 8°. The two fiber components are no longer apparent with the QB-ODF approximation (see Fig. 2(e)). These exemplary simulations indicate that DK-ODF is capable of resolving fiber crossing at angles as small as 2° for two fiber configurations - however the offset to the true orientation in this case reached 18°. The offset decreases as the angle of separation increases. As the number of fiber directions increases, the DK-ODF approximation

appears to resolve orthogonal or close to orthogonal fiber configurations (as illustrated in Fig. l(b)). Offsets of the exemplary ODF peaks with respect to the component fiber directions are also apparent at small intersection angles for the exact ODF.

Exemplary Brain Imaging Experiments

[0080] An exemplary DK approximation was used to derive ODF maps of the in vivo brain imaging data. Similar results were obtained for all subjects. Figs. 3-5 show the absolute and min-max normalized DK-derived NG-ODF maps and the corresponding DT-ODF maps for several brain regions where complex fiber architecture is present. Voxels with multiple fiber components can be distinguished on the DK-ODF maps. In general, the min-max normalization can improve the visualization of the ODF peaks. The fiber orientations resolved using the DK approximation are consistent with known anatomy. Complex fiber architecture is not apparent on the DT-ODF maps.

[0081] Figs. 3(a)-3(e), 4(a)-4(e) and 5(a)-5(d) show exemplary ODF maps of an axial slice situated at the cerebral pons level. Such exemplary region contains several fiber populations including the superiorly – inferiorly oriented pyramidal and central tegmental tracts and the transverse pontine fibers that are running from left to right. For example, Fig. 3(a) illustrates an exemplary DT approximation, Fig. 3(b) illustrates an exemplary DK-derived NG-ODF, and Fig. 3(c) illustrates an exemplary min-max scaled version of Fig. 3(b). An exemplary DT derived color map of the same axial slice and location of the ODF maps are illustrated in Fig. 3(d). Fiber directions obtained using the DK (left - unsealed ODF and center – min-max scaled ODF) and DT (right) approximations for one voxel with apparent partial volume averaging of two fiber populations are illustrated, as an example,in Fig. 3(e).

[0082] Two fiber directions (transverse and superior-inferior) are shown in regions with mixed fiber populations (see Figs. 3(b) and 3(c)); these fiber directions appear to be in agreement with known anatomy. The DT approximation does not only fail to resolve the two fiber populations in voxels affected by partial volume averaging, but appears to fail to describe either orientation correctly (e.g., see Fig 3(e)).

[0083] Figs. 4(a)-4(e) show exemplary intersections of the superior longitudinal fasciculus (SLF), corona radiata, and corpus callosum in the centrum semiovale region. For example, Fig. 4(a) illustrates an exemplary DT approximation, Fig. 4(b) illustrates an exemplary DK-derived NG-ODF, and Fig. 4(c) illustrates an exemplary min-max scaled version of Fig. 4(b). An exemplary color map in Fig. 4(d) illustrates a position of the ODF maps with respect to other brain structures. Fig. 4(e) illustrates exemplary ODFs and corresponding fiber directions for a voxel where three distinct fiber populations are apparent using the DK approximation. Exemplary regions with two and three fiber populations are illustrated on the DK-ODF map. On the DK-ODF map, the SLF runs continuously in the anterior-posterior direction, whereas it is interrupted on the color map which was obtained using the exemplary DT-ODF approximation.

[0084] Figs. 5(a)-5(d) illustrate exemplary ODF maps of the intersection between the posterior region of the superior longitudinal fasciculus with the projection fibers of the corona radiata and the posterior transverse association fibers for acquisition. For example, Fig. 5(a) illustrates an exemplary DT approximation, Fig. 5(b) illustrates an exemplary DK-derived NG-ODF (min-max scaled), Fig. 5(c) illustrates an exemplary DT-derived color map that shows the position of the magnified views with respect to other brain structures, and Fig. 5(d) illustrates exemplary fiber directions obtained using the DK (left -unsealed ODF and center — min-max scaled ODF) and DT (right) approximations for

several voxels. Voxels with two-fiber populations are also shown in the DK-ODF maps illustrating regions where the posterior SLF interfaces with either corona radiata or transverse association fibers running from left to right. The ODF shows changes in shape and orientation as it represents either mixtures of fibers running anteriorly-posteriorly and vertically oblique or mixtures of fibers oriented anteriorly-posteriorly and from right to left, as illustrated, as example, in Figs. 5(b) and 5(c).

Exemplary Parametric Maps

[0085] Figs. 6(a)-6(d) are illustrations of exemplary brain images of a mean diffusivity, axial diffusivity, radial diffusivity and a fractional anisotropy, respectively, provided by conventional diffusion tensor imaging. The data can be obtained using a, e.g., magnetic resonance imaging scanner. For example, the mean diffusivity illustrated in Fig. 6(a) can be derived, e.g., using Eq. [6]. The axial diffusivity illustrated in Fig. 6(b) can be derived, e.g., using Eq. [10]. The radial diffusivity illustrated in Fig. 6(c) can be derived, e.g., using Eq. [11], and the fractional anisotropy illustrated in Fig. 6(d) can be derived, e.g., using Eq. [12]. The mean, axial, and radial diffusivities, provided in Figs. 6(a) – 6(c), respectively, and the fractional anisotropy provided in Fig. 6(d) are similar to what can be generated with conventional diffusion tensor imaging. Calibration bars shown in these figures are in units of $\mu m^2/ms$ for the mean, axial, and radial diffusivities, and calibration bars can be dimensionless for the fractional anisotropy.

[0086] Figs. 7(a)-7(c) are illustrations of exemplary parametric maps derived with real-time diffusional kurtosis imaging for a single axial brain slice using an exemplary embodiment of the present disclosure. The mean, axial, and radial kurtoses, as illustrated in Figs. 7(a)-7(c), respectively, can be exemplary metrics provided by DKI. The mean kurtosis illustrated in Fig. 7(a) can be derived, e.g., using Eq. [13]. The axial kurtosis

illustrated in Fig. 7(b) can be derived, e.g., using Eq. [20], and the radial kurtosis illustrated in Fig. 7(c) can be derived, e.g., using Eq. [21]. Calibration bars can be dimensionless for the mean, axial, and radial kurtoses illustrated in Figs. 7(a)-7(c), respectively.

Further Details of Exemplary Embodiments

[0087] An exemplary ODF reconstruction procedure based on the DK approximation of the diffusion signal is described herein. The fiber crossing simulation results support the ability of the DK-ODF approximation to resolve multiple volume averaged fibers. The technique can estimate the directionality for mixtures of two, three or four intersecting fibers. The offset between the true and the estimated fiber directions that is observed for fibers intersecting at a small angle is characteristic to other HARDI techniques and is provided by the ODF model. This can be due to adherence between the closely situated peaks on the ODF.

[0088] The exemplary simulations included use analytical representations of the diffusion probability distribution function and the ODFs, and may not model the influence of the imaging acquisition scheme and signal-to-noise ratio.

[0089] The DK-ODF maps of the brain anatomy can correspond to the current knowledge of white matter fiber architecture. Configurations with both two and three crossing fibers as well as unidirectional voxels are all apparent on the ODF maps.

[0090] One of the exemplary advantages of DKI is that can use low b values ($b < 2500$ s/mm2). This can result in diffusion-weighted images with relatively higher signal to noise ratio compared to the signal-to-noise ratio of images used by other ODF techniques. Moreover, the exemplary DK approximation can include only the lower moments of the

water diffusion distribution (up to the forth order), thus retaining only the low frequency components of the ODF spherical harmonic spectrum. Additional smoothing may be also introduced by the linearization of the signal in the kurtosis coefficient K that is used to derive the ODF approximation and by using the diffusion and kurtosis tensors to estimate the diffusion and kurtosis coefficients used in the Funk-Radon transform. Consequently, the reconstructed ODFs can be inherently smooth, and do not require further regularization (e.g., spherical convolution), which is usually employed by other ODF techniques. Further, the exemplary derivation of the diffusion and kurtosis tensor employed by DK-ODF can use a limited number of measurements.

[0091] An alternative exemplary approach for obtaining directional information in regions with complex fiber architecture is to use q-space imaging (QSI) techniques to extract the full diffusion displacement probability distribution. However, the QSI techniques require a large number of samples and high b values, thus resulting in long imaging times and images with low signal to noise ratio. Further, the DK-ODF model, in contrast with the QBI-ODF approximations, has no explicit b- value dependence.

Exemplary Embodiments of Methods, Systems and Computer-Accessible Medium

[0092] Fig. 8 illustrates a flow diagram according to an exemplary embodiment of a method of an exemplary real-time diffusional kurtosis imaging according to the present disclosure. For example, in 510, data can be acquired, e.g., using a diffusion-weighted imaging MRI sequence with 3 b-values and 15 or more diffusion directions. At 520, the diffusion D and kurtosis K can be calculated for each diffusion direction. Such calculation can be provided, e.g., using the analytic formulae of Eqs. [1]-[3]. At 530, linear systems, as exemplified by Eqs. [4] and [5], can be solved for the diffusion tensor DT and kurtosis tensor KT. At 540, the method can rotate to eigenframes that

diagonalizes the diffusion tensor, by applying any of several exemplary standard techniques, such as Jacobi's method.. Lastly, at 550, analytic formulae or procedures can be used to calculate the desired diffusion metrics, such as mean, axial and radial diffusivities and mean, axial and radial kurtoses. The mean, axial, and radial diffusivities can be derived using Eqs. [6], [10], and [11]. The mean, axial, and radial kurtoses can be derived using Eqs. [13], [20], and [21]. Such diffusion metrics can provide for real-time diffusional kurtosis imaging.

[0093] Fig. 9 illustrates a flow diagram of an exemplary method for determining a measure of a diffusional kurtosis according to an exemplary embodiment of the present disclosure. Initially, e.g., at procedure 610, an image can be obtained of an anatomical structure, such as a portion of a brain of a subject, such as a human subject. This exemplary image can be provided by several different methods or procedures, such as, e.g., by MRI. A diffusion weighted image of the image can be provided at procedure 620. The diffusion weighted image can be acquired for three or more b-values, and can be acquired for 15 or more gradient directions. Data can then be received relating to the diffusion weighted image at 630.

[0094] At procedure 640, a measure of a diffusional kurtosis can be determined. This diffusional kurtosis can be measured using a closed form solution at procedure 650, as described above. The measure of the diffusional kurtosis can be determined using a mean kurtosis as well, which can be determined by averaging measures of a diffusion and a kurtosis over each gradient direction. The measure of the diffusional kurtosis can also be an axial kurtosis or a radial kurtosis.

[0095] Using the measure of the diffusional kurtosis, an orientation distribution function can be determined at procedure 660. One or more fiber crossings can be resolved using

the orientation distribution function at procedure 670. The fiber crossing can be a crossing of two, three or four fibers, or more. Further, a medical condition of the subject can be evaluated using the measure of the diffusional kurtosis at procedure 680, such as Alzheimer's disease, stroke, head trauma, attention deficit hyperactivity disorder or schizophrenia. A measure of diffusional restrictivity can also be determined using the measure of the diffusional kurtosis, at procedure 690.

[0096] Fig. 10 illustrates a block diagram of an exemplary embodiment of a system according to the present disclosure. For example, a computer 700 can be provided which can have a processor 730 that can be configured or programmed to perform the exemplary steps and/or procedures of the exemplary embodiments of the techniques described above, and those as described herein with respect to the exemplary procedure shown in Fig. 9. For example, a subject/specimen 710 can be positioned and an anatomical region of interest can be selected on the subject/specimen 710, as provided for in procedure 610 above. The imaging device 720 can be used to obtain data for one or more images of the anatomical region of interest. The data/images (e.g., diffusion weighted images) can be provided from the imaging device 720 to the computer 700, which can be transmitted to the processor 730 and/or storage arrangement 740.

[0097] According to one exemplary embodiment of the present disclosure, the data can be stored in a storage arrangement 740 (e.g., hard drive, memory device, such as RAM, ROM, memory stick, floppy drive, etc.). The processor 730 can access the storage arrangement 740 to execute a computer program or a set of instructions (stored on or in the storage arrangement 740) which perform the procedures according to the exemplary embodiments of the present invention. Thus, e.g., when the processor 730 performs such instructions and/or computer program, the processor 730 can be configured to perform the

exemplary embodiments of the procedures according to the present invention, as described above herein.

[0098] For example, the processor 730 can be programmed to receive data relating to at least one diffusion weighted image, and determine a measure of a diffusional kurtosis as a function of the received data. This information can be received directly from the imaging device 720 or accessed from the storage arrangement 740. The processor 730 can also be programmed to determine information for measuring a diffusional kurtosis, and can then resolve one or more fiber crossings, evaluate a medical condition of the subject, and/or measure a diffusion restrictivity.

[0099] A display 750 can also be provided for the exemplary system of Fig. 7. The storage arrangement 740 and the display 750 can be provided within the computer 700 or external from the computer 700. For example, the information received by the processor 730 and the information determined by the processor 730, as well as the information stored on the storage arrangement 740 can be displayed on the display 750 in a user-readable format.

[00100] The foregoing merely illustrates the principles of the invention. Various modifications and alterations to the described embodiments will be apparent to those skilled in the art in view of the teachings herein. It will thus be appreciated that those skilled in the art will be able to devise numerous systems, arrangements, and methods which, although not explicitly shown or described herein, embody the principles of the invention and are thus within the spirit and scope of the invention. In addition, all publications and references referred to above are incorporated herein by reference in their entireties. It should be understood that the exemplary procedures described herein can be stored on any computer accessible medium, including a hard drive, RAM, ROM,

removable discs, CD-ROM, memory sticks, etc., and executed by a processing arrangement which can be a microprocessor, mini, macro, mainframe, etc.

WHAT IS CLAIMED IS:

1. A method for determining a measure of diffusional kurtosis, comprising:

receiving data relating to at least one diffusion weighted image; and

using a computer arrangement, determining a measure of a diffusional kurtosis as a function of the received data using a closed form solution procedure.

2. The method of claim 1, further comprising performing at least one of (i) providing the measure of the diffusional kurtosis to a display device, or (ii) recording the measure of the diffusional kurtosis.

3. The method of claim 1, wherein the at least one diffusion weighted image is acquired for three or more b-values.

4. The method of claim 3, wherein the at least one diffusion weighted image is acquired for 15 or more gradient directions.

5. The method of claim 1, wherein the at least one diffusion weighted image is acquired for three b-values.

6. The method of claim 1, wherein the measure of the diffusional kurtosis is determined using a mean kurtosis procedure.

7. The method of claim 6 wherein the mean kurtosis is determined by averaging measures of a diffusion and a kurtosis over each gradient direction.

8. The method of claim 1, wherein the closed form solution procedure includes at least one or more elliptic integrals.

9. The method of claim 8, wherein the one or more elliptic integrals are associated with eigenvalues of at least one diffusion tensor based on the at least one diffusion weighted image.

10. The method of claim 8, wherein the at least one or more elliptic integrals are associated with at least one Carlson symmetric form of an elliptic integral.

11. The method of claim 1, wherein the measure of the diffusional kurtosis is at least one of an axial kurtosis or a radial kurtosis.

12. The method of claim 1, wherein at least a portion of the received data relates to at least one orientation distribution function, the portion of the received data being calculated using the measure of the diffusional kurtosis.

13. The method of claim 12, further comprising resolving at least one fiber crossing using the received data from the at least one orientation distribution function.

14. The method of claim 13, wherein the at least one fiber crossing is a crossing of at least one of two fibers, three fibers or four fibers.

15. The method of claim 13, further comprising providing a directional color map of the at least one fiber crossing, wherein the directional color map provides fiber direction

estimates as a function of the data associated with the at least one orientation distribution function.

16. The method of claim 15, further comprising performing a fiber tractography using the data associated with the at least one orientation distribution function.

17. The method of claim 16, further comprising analyzing white matter connectivity patterns using the data associated with the at least one orientation distribution function.

18. The method of claim 16, further comprising estimating white matter pathways using the data associated with the at least one orientation distribution function.

19. The method of claim 16, further comprising analyzing fibers tracts which at least one of cross, kiss, branch, merge or splay, using the data associated with the at least one orientation distribution function.

20. The method of claim 12, wherein the received data associated with the at least one orientation distribution function includes Gaussian diffusion contributions and substantially excludes non-Gaussian diffusion contributions.

21. The method of claim 12, wherein the data associated with the at least one orientation distribution function includes non-Gaussian diffusion contributions and substantially excludes Gaussian diffusion contributions.

22. The method of claim 12, wherein the data associated with the at least one orientation distribution function includes Gaussian diffusion contributions and non-Gaussian diffusion contributions.

23. The method of claim 12, wherein the data associated with the at least one orientation distribution function is an approximation of an integral of a function depending on diffusion and kurtosis coefficients over a perpendicularly-oriented great circle.

24. The method of claim 1, further comprising assessing at least one medical condition of a subject using the measure of the diffusional kurtosis.

25. The method of claim 24, wherein the at least one medical condition is at least one of a neurological disease or a neuro-degenerative diseases.

26. The method of claim 24, wherein the at least one medical condition is at least one of Alzheimer's disease, stroke, head trauma, attention deficit hyperactivity disorder or schizophrenia.

27. The method of claim 24, wherein the at least one medical condition is assessed by comparing further data relating to the subject with predetermined control data.

28. The method of claim 27, wherein the control data comprises age-matched control data.

29. The method of claim 1, further comprising determining a measure of a diffusional restrictivity using the measure of the diffusional kurtosis.

30. The method of claim 29, wherein the measure of the diffusional restrictivity is determined from a diffusion tensor and a kurtosis tensor relating to the at least one diffusion weighted image.

31. The method of claim 29, wherein the measure of the diffusional restrictivity includes a measure of Gaussian restrictivity which substantially excludes non-Gaussian restrictivity.

32. The method of claim 29, wherein the measure of the diffusional restrictivity includes a measure of non-Gaussian restrictivity which substantially excludes Gaussian restrictivity.

33. The method of claim 29, wherein the measure of the diffusional restrictivity includes a measure of Gaussian restrictivity and non-Gaussian restrictivity.

34. The method of claim 29, wherein the measure of diffusional restrictivity is determined using a first measure dependent on diffusivity and a second measure dependent on diffusional kurtosis.

35. The method of claim 34, wherein the second measure reflects non-Gaussian diffusion contributions to a diffusion signal.

36. The method of claim 29, further comprising identifying at least one region of interest in an anatomical structure based on at least one of the measure of the diffusional kurtosis or the measure of the diffusional restrictivity.

37. The method of claim 36, wherein the anatomical structure comprises a brain tissue.

38. The method of claim 36, wherein the at least one region of interest indicates differences in microstructure between different portions of the anatomical structure.

39. The method of claim 36, wherein the at least one region of interest at least partially distinguishes between a reversibly injured tissue and an irreversibly injured tissue.

40. A system for determining a measure of diffusional kurtosis comprising:

a first arrangement configured to receive data relating to at least one diffusion weighted image; and

a second arrangement configured to determine a measure of a diffusional kurtosis as a function of the received data using a closed form solution procedure.

41. The system of claim 40, wherein the second arrangement is further configured to perform at least one of (i) provide the measure of the diffusional kurtosis to a display device, or (ii) record the measure of the diffusional kurtosis.

42. The system of claim 40, wherein the at least one diffusion weighted image is acquired for three or more b-values.

43. The system of claim 42, wherein the at least one diffusion weighted image is acquired for 15 or more gradient directions.

44. The system of claim 40, wherein the at least one diffusion weighted image is acquired for three b-values.

45. The system of claim 40, wherein the measure of the diffusional kurtosis is determined using a mean kurtosis procedure.

46. The system of claim 45, wherein the mean kurtosis is determined by averaging measures of a diffusion and a kurtosis over each gradient direction.

47. The system of claim 40, wherein the measure of the diffusional kurtosis is at least one of an axial kurtosis and a radial kurtosis.

48. The system of claim 40, wherein at least a portion of the received data relates to at least one orientation distribution function, the portion of the received data being calculated using the measure of the diffusional kurtosis.

49. The system of claim 40, wherein the second arrangement is further configured to assess at least one medical condition of a subject using the measure of the diffusional kurtosis.

50. The system of claim 49, wherein the at least one medical condition is at least one of a neurological disease or a neuro-degenerative diseases.

51. The system of claim 49, wherein the at least one medical condition is at least one of Alzheimer's disease, stroke, head trauma, attention deficit hyperactivity disorder or schizophrenia.

52. The system of claim 49, wherein the at least one medical condition is assessed by comparing further data relating to the subject with predetermined control data.

53. The system of claim 52, wherein the control data comprises age-matched control data.

54. The system of claim 40, wherein the second arrangement is further configured to determine a measure of a diffusional restrictivity using the measure of the diffusional kurtosis.

55. The system of claim 54, wherein the measure of the diffusional restrictivity is determined from a diffusion tensor and a kurtosis tensor relating to the at least one diffusion weighted image.

56. The system of claim 54, wherein the measure of the diffusional restrictivity includes a measure of Gaussian restrictivity which substantially excludes non-Gaussian restrictivity.

57. The system of claim 54, wherein the measure of the diffusional restrictivity includes a measure of non-Gaussian restrictivity which substantially excludes Gaussian restrictivity.

58. The system of claim 54, wherein the measure of the diffusional restrictivity includes a measure of Gaussian restrictivity and non-Gaussian restrictivity.

59. The system of claim 54, wherein the measure of the diffusional restrictivity is determined using a first measure dependent on diffusivity and a second measure dependent on diffusional kurtosis.

60. The system of claim 59, wherein the second measure reflects non-Gaussian diffusion contributions to a diffusion signal.

61. The system of claim 54, wherein the second arrangement is further configured to identify at least one region of interest in an anatomical structure based on at least one of the measure of the diffusional kurtosis or the measure of the diffusional restrictivity.

62. The system of claim 61, wherein the anatomical structure comprises a brain tissue.

63. The system of claim 61, wherein the at least one region of interest indicates differences in microstructure between different portions of the anatomical structure.

64. The system of claim 61, wherein the at least one region of interest at least partially distinguishes between a reversibly injured tissue and an irreversibly injured tissue.

65. A computer-accessible medium for determining a measure of diffusional kurtosis, the computer-accessible medium including instructions thereon, wherein, when a computing arrangement executes the instructions, the computing arrangement is configured to perform procedures comprising:

receiving data relating to at least one diffusion weighted image; and

determining a measure of a diffusional kurtosis as a function of the received data using a closed form solution procedure.

66. The computer-accessible medium of claim 65, wherein the computing arrangement is further configured to at least one of (i) provide the measure of the diffusional kurtosis to a display device, or (ii) record the measure of the diffusional kurtosis.

67. The computer-accessible medium of claim 65, wherein the at least one diffusion weighted image is acquired for three or more b-values.

68. The computer-accessible medium of claim 67, wherein the at least one diffusion weighted image is acquired for 15 or more gradient directions.

69. The computer-accessible medium of claim 65, wherein the at least one diffusion weighted image is acquired for three b-values.

70. The computer-accessible medium of claim 65, wherein the measure of the diffusional kurtosis is determined using a mean kurtosis procedure.

71. The computer-accessible medium of claim 70, wherein the mean kurtosis is determined by averaging measures of a diffusion and a kurtosis over each gradient direction.

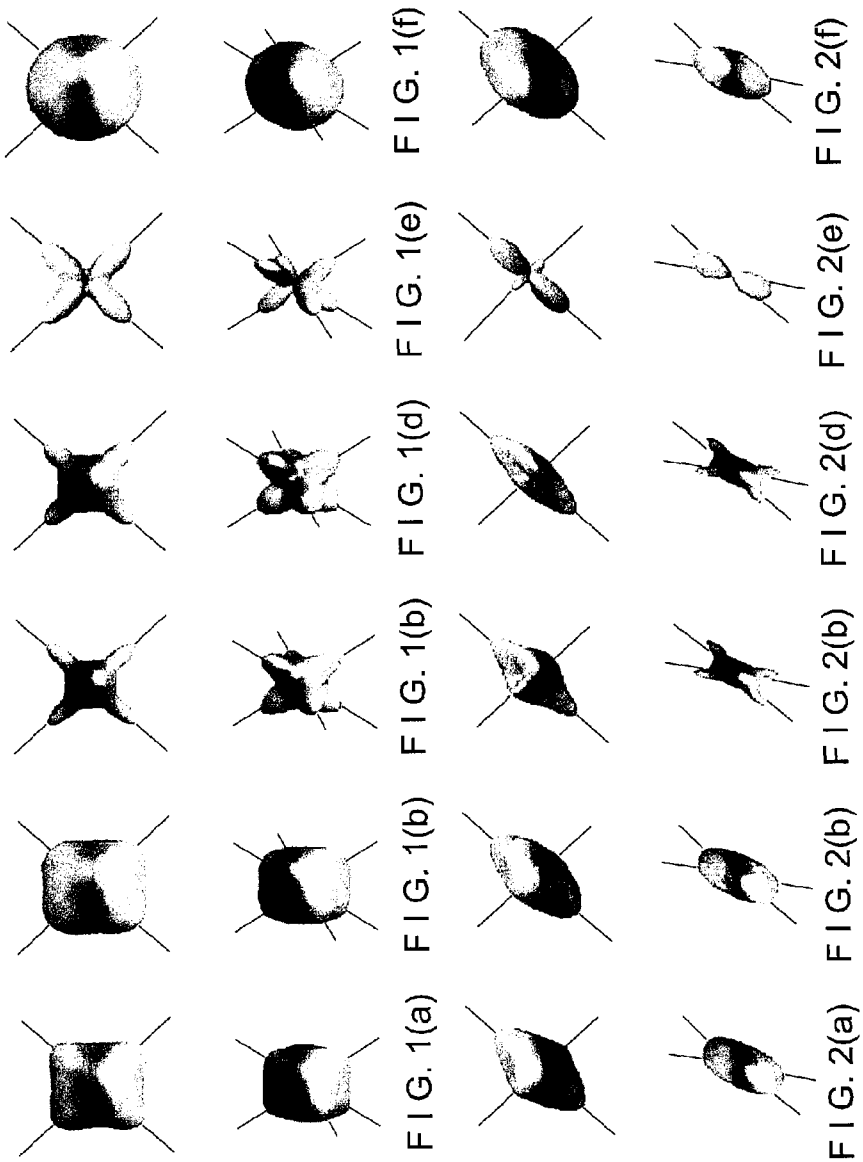
FIG. 1(f)
FIG. 2(f)
FIG. 1(e)
FIG. 2(e)
FIG. 1(d)
FIG. 2(d)
FIG. 1(b)
FIG. 2(b)
FIG. 1(b)
FIG. 2(b)
FIG. 1(a)
FIG. 2(a)

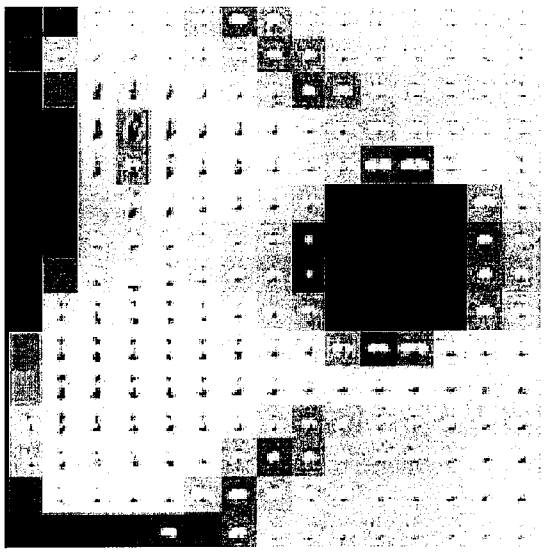

FIG. 3(b)

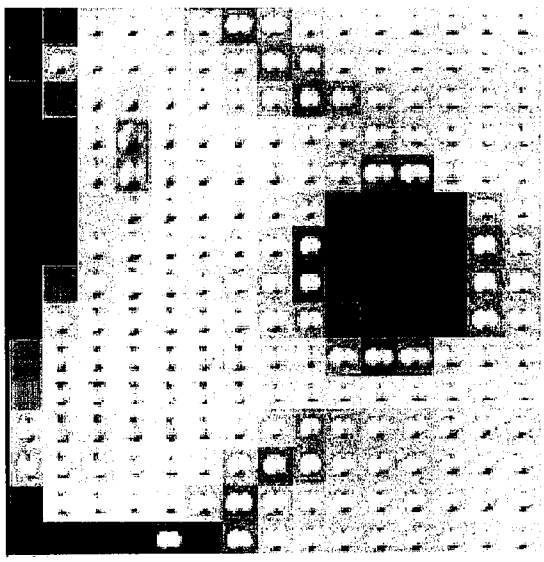

FIG. 3(a)

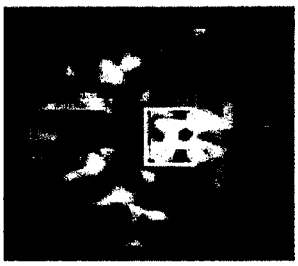

FIG. 3(d)

FIG. 3(e)

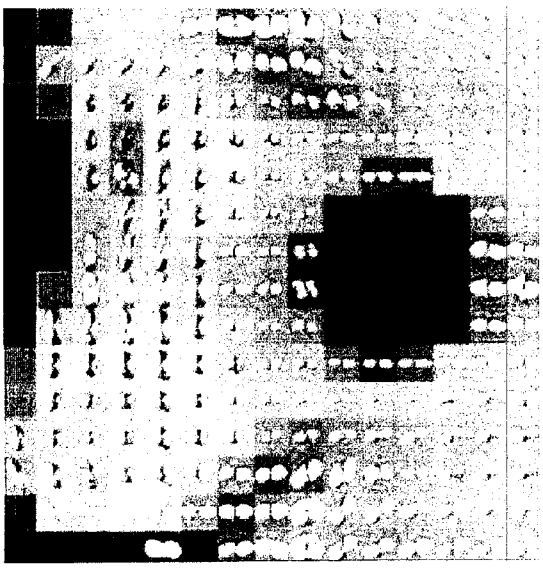

FIG. 3(c)

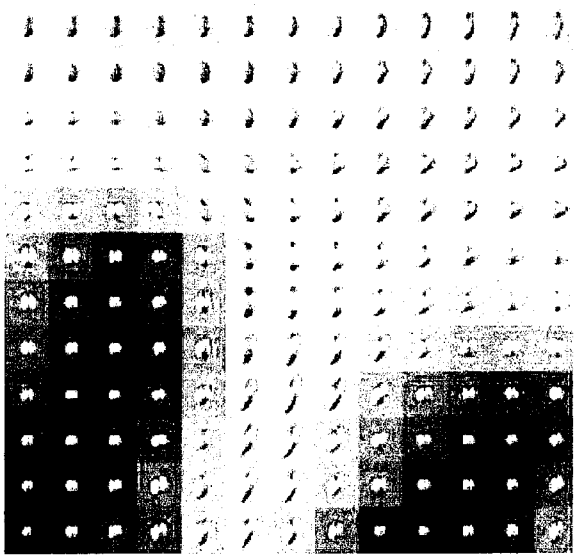

FIG. 4(b)

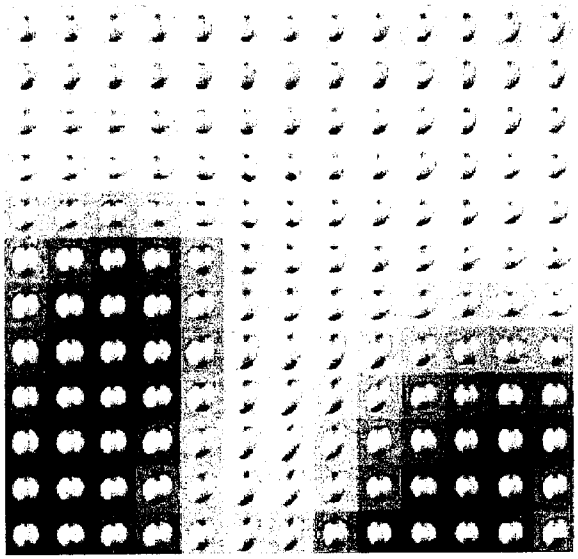

FIG. 4(a)

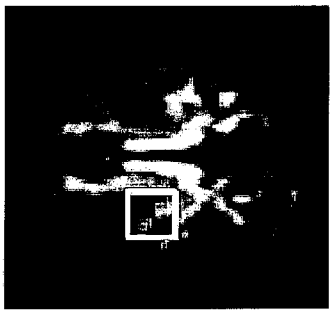

FIG. 4(d)

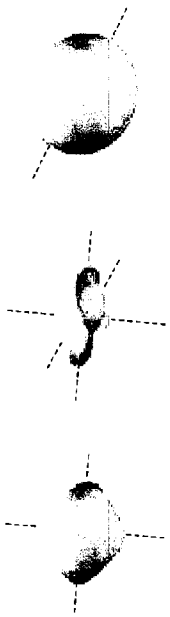

FIG. 4(e)

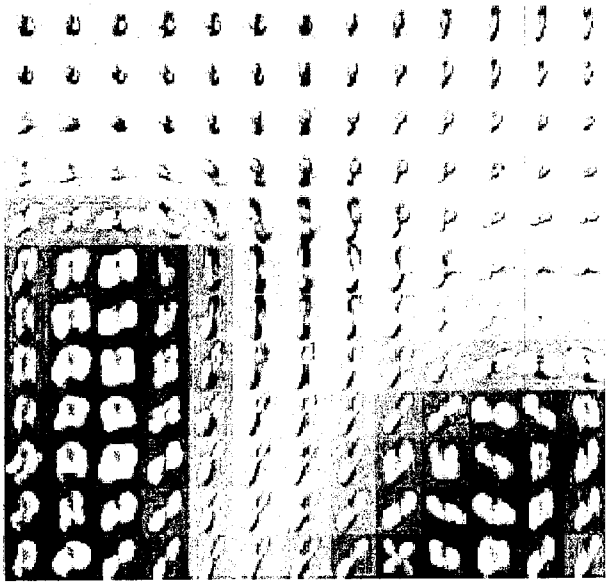

FIG. 4(c)

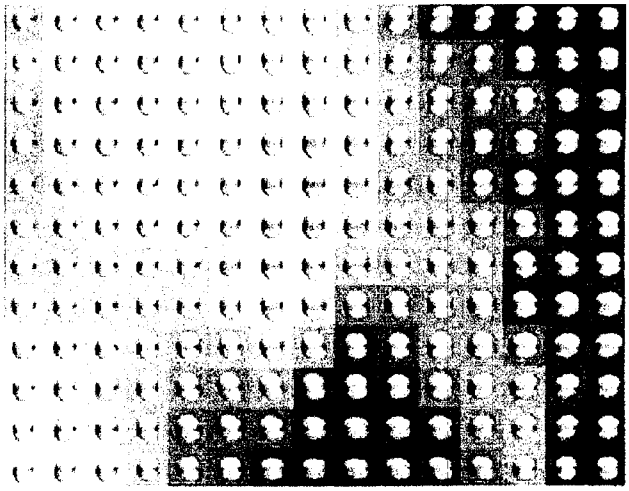

FIG. 5(a)

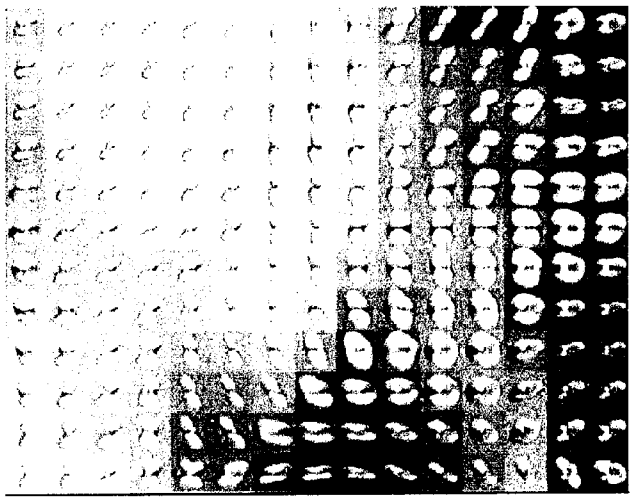

FIG. 5(b)

F I G. 5(c)

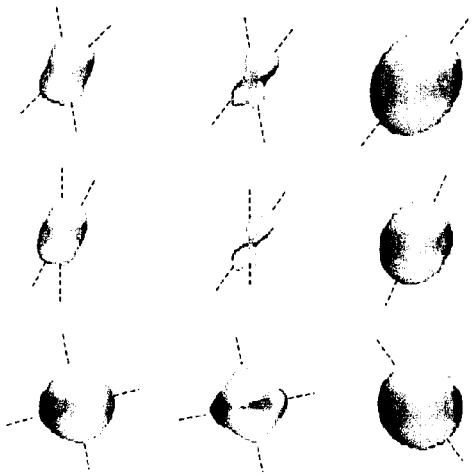

F I G. 5(d)

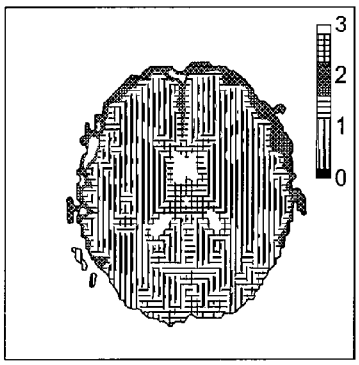

FIG. 6(a)

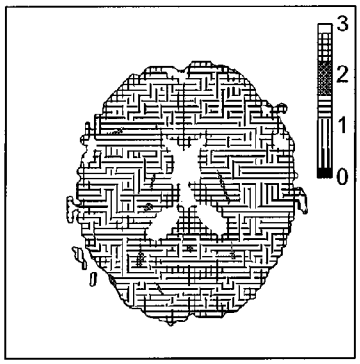

FIG. 6(b)

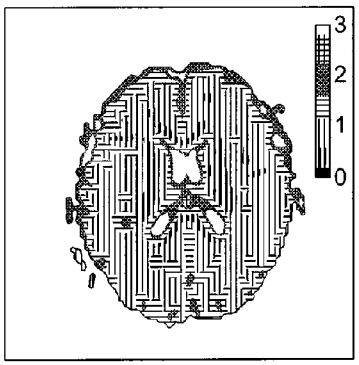

FIG. 6(c)

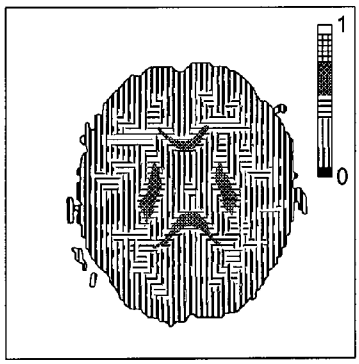

FIG. 6(d)

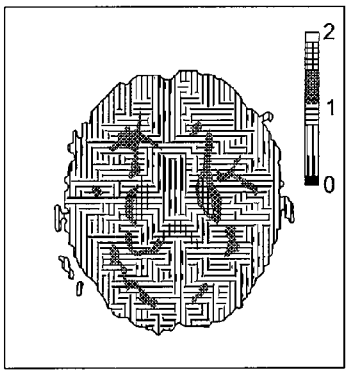

F I G. 7(a)

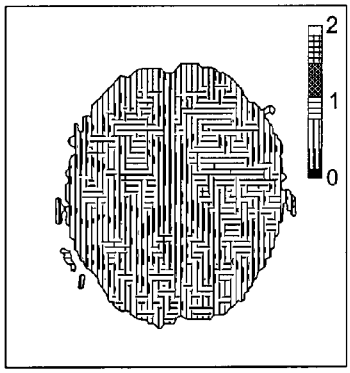

F I G. 7(b)

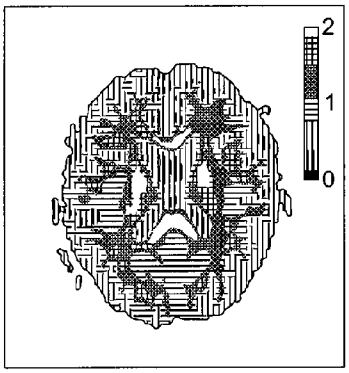

F I G. 7(c)

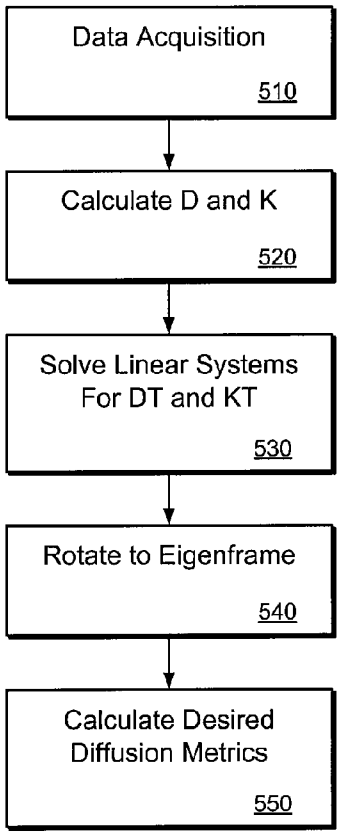
Data Acquisition
510
Calculate D and K
520
Solve Linear Systems For DT and KT
530
Rotate to Eigenframe
540
Calculate Desired Diffusion Metrics
550

FIG. 8

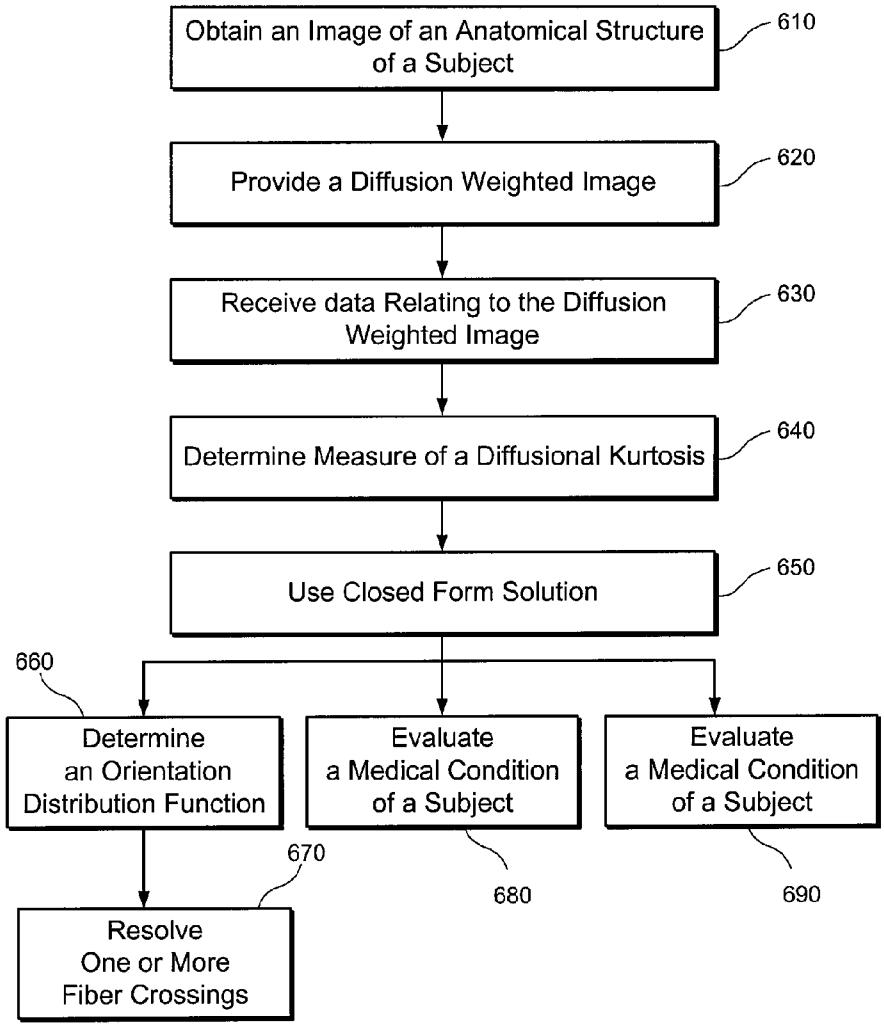
Obtain an Image of an Anatomical Structure of a Subject
610
Provide a Diffusion Weighted Image
620
Receive data Relating to the Diffusion Weighted Image
630
Determine Measure of a Diffusional Kurtosis
640
Use Closed Form Solution
650
660
Determine an Orientation Distribution Function
Evaluate a Medical Condition of a Subject
Evaluate a Medical Condition of a Subject
670
680
690
Resolve One or More Fiber Crossings

FIG. 9

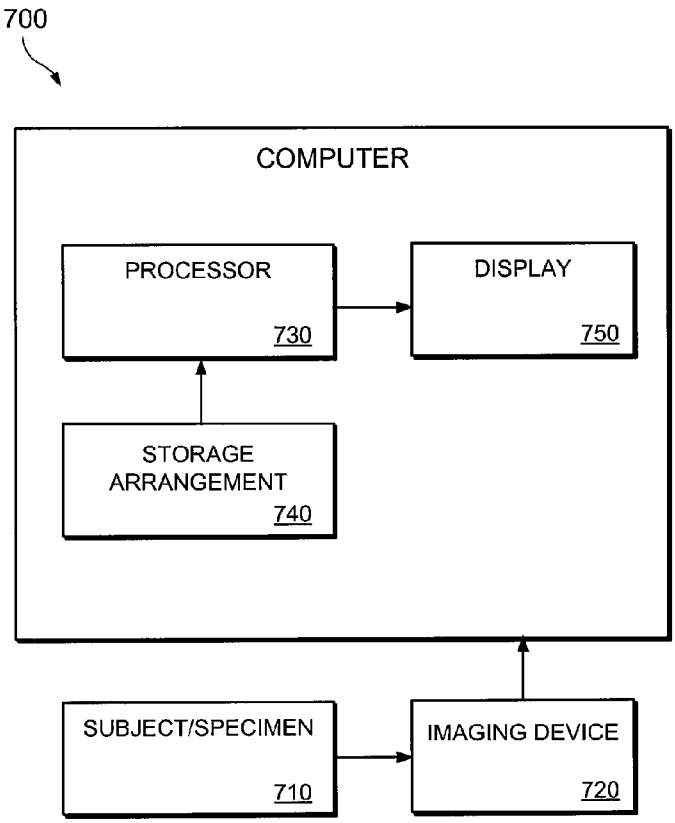
700
COMPUTER
PROCESSOR
730
DISPLAY
750
STORAGE
ARRANGEMENT
740
SUBJECT/SPECIMEN
710
IMAGING DEVICE
720

F I G. 10